Structure of Human Synaptotagmin 1 C2AB in the Absence of Ca^{2+} Reveals a Novel Domain Association[†,‡]

Kerry L. Fuson,[§] Miguel Montes,[∥] J. Justin Robert,[⊥] and R. Bryan Sutton*[,∥,⊥]

Departments of Biochemistry and Molecular Biology and of Neuroscience and Cell Biology and Sealy Center for Structural Biology and Molecular Biophysics, The University of Texas Medical Branch, Galveston, Texas 77555

Received August 15, 2007; Revised Manuscript Received September 17, 2007

ABSTRACT: Release of neurotransmitter from synaptic vesicles requires the Ca^{2+}/phospholipid-binding protein synaptotagmin 1. There is considerable evidence that cooperation between the tandem C2 domains of synaptotagmin is a requirement of regulated exocytosis; however, high-resolution structural evidence for this interaction has been lacking. The 2.7 Å crystal structure of the cytosolic domains of human synaptotagmin 1 in the absence of Ca^{2+} reveals a novel closed conformation of the protein. The shared interface between C2A and C2B is stabilized by a network of interactions between residues on the C-terminal α-helix of the C2B domain and residues on loops 1−3 of the Ca^{2+}-binding region of C2A. These interactions alter the overall shape of the Ca^{2+}-binding pocket of C2A, but not that of C2B. Thus, synaptotagmin 1 C2A−C2B may utilize a novel regulatory mechanism whereby one C2 domain could regulate the other until an appropriate triggering event decouples them.

Ca^{2+}-dependent release of neurotransmitter into the synaptic space is one of the fundamental tenets of modern neurobiology. This aspect of neuronal function has been studied for many years, yet the molecular details are only now being elucidated. The process begins with a neurotransmitter-filled synaptic vesicle progressing from a docked position to a primed, fusion-competent position next to the target membrane. Once the vesicle membrane and the target membrane fuse, neurotransmitter is released into the synaptic space. The merger of these two distinct bilayers, and the concomitant formation of a lipidic fusion pore, is mediated by Ca^{2+} and a number of proteins specific for the task. These include the protein complex formed between vesicle-localized R-SNAREs[1] such as synaptobrevin and the Q-SNAREs such as SNAP-25 and syntaxin. This protein complex either acts as a staging platform for other constituents required for vesicle fusion (*1*) or may directly participate in the actual fusion event itself (*2*). Regardless of the specific mechanism, the fusion of vesicle membranes with presynaptic membranes requires a calcium ion sensor or trigger. The C2A−C2B domains of synaptotagmin 1 (Syt1) possess the Ca^{2+}-dependent phospholipid-binding activity (*3*) and the SNARE-binding activity predicted for such a trigger (*4*).

Syt1 is a vesicle-localized transmembrane protein with two tandem C2 domains (C2A and C2B) at the C-terminus of the protein. There are two possible explanations for the tandem C2 domain architecture of Syt1. Either the two domains are joined by a flexible linker and are completely independent or there is some degree of cooperativity between the domains that is essential to the overall function of the protein. These two scenarios are not mutually exclusive, as evidence exists for both. NMR analysis of Syt1 C2A−C2B concluded that there was no detectable interaction between the domains (*5*). Also, the crystal structure of Syt3, a homologue of Syt1, displays no evidence of interdomain interaction (*6*) (Figure 1B). On the other hand, the C2 domains of Syt1 are known to function synergistically when compared to isolated C2 domains (*7*). Subsequent experiments concluded that a close physical coupling of the tandem domains is critical for function (*8*).

Each C2 domain of synaptotagmin 1 is formed from eight β-strands arranged around a Greek key topology, known as the C2 key (*9*). The curvature of the domains is governed by a series of tandem β-bulges, some of which are unique to the C2 domain. Both the C2A and C2B domains of Syt1 have extended loops at one end of the domain (loops 1−3) that have been specialized for Ca^{2+}/phospholipid binding (*10*). Three ions can bind in a cuplike depression formed from these loops, but only loops 1 and 3 contribute calcium ion-binding residues. Loop 2 contributes to the overall shape of the Ca^{2+}-binding pocket, but does not directly participate

[†] This work was supported by NIH Grant MH-070589 to R.B.S. R.B.S. is also supported by a Career Award in the Biomedical Sciences from the Burroughs-Wellcome Fund. K.L.F. was supported by a training fellowship from the Houston Area Molecular Biophysics Program. Portions of this research were carried out at the Stanford Synchrotron Radiation Laboratory (SSRL), a national user facility operated by Stanford University on behalf of the U.S. Department of Energy, Office of Basic Energy Sciences. The SSRL Structural Molecular Biology Program is supported by the Department of Energy, Office of Biological and Environmental Research, and by the National Institutes of Health, National Center for Research Resources, Biomedical Technology Program, and National Institute of General Medical Sciences.

[‡] Coordinates and structure factors have been deposited in the Protein Data Bank under the accession number 2R83.

* To whom correspondence should be addressed. E-mail: rbsutton@utmb.edu. Fax: (409) 747-2187. Phone: (409) 772-1305.

[§] Department of Biochemistry and Molecular Biology.

[∥] Department of Neuroscience and Cell Biology.

[⊥] Sealy Center for Structural Biology and Molecular Biophysics.

[1] Abbreviations: ASU, asymmetric unit; EPR, electron paramagnetic resonance; GST, glutathione S-transferase; H-bond, hydrogen bond; NMR, nuclear magnetic resonance; PCR, polymerase chain reaction; SNARE, SNAP receptor; Syt, synaptotagmin.

10.1021/bi701651k CCC: $37.00
Published on Web 10/23/2007

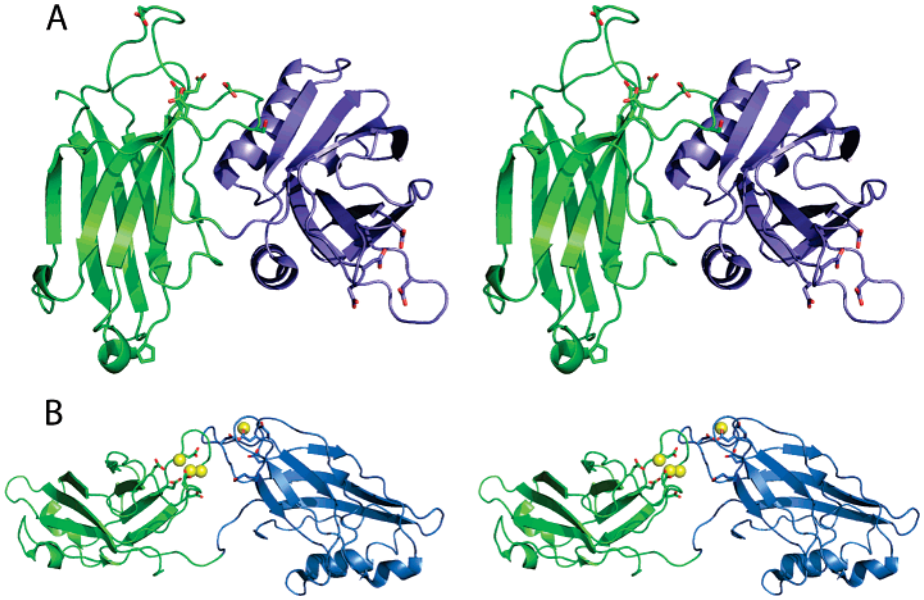

FIGURE 1: Open and closed conformations of synaptotagmin. (A) Stereoview of Syt1 C2A−C2B in the closed configuration. The C2A domain is colored as green ribbons. The C2B domain is colored as blue ribbons. The six known Ca^{2+}-binding residues are shown as sticks. (B) Stereodiagram of synaptotagmin 3 C2A−C2B in the open configuration (PDB code 1DQV). The C2A domain in Syt3 is rendered as green ribbons. The C2B domain in Syt3 is rendered as blue ribbons. Yellow spheres represent magnesium ions.

in the coordination of cations. Hydrophobic residues at the apexes of loop 1 and loop 3 embed the domain in the target membrane (*11*, *12*). In the isoforms of Syt that bind Ca^{2+}, five conserved acidic residues on loops 1 and 3 coordinate the binding of Ca^{2+}. Both X-ray studies and NMR analysis of the cation-binding properties of the Syt1 C2A domain confirm that the C2A domain can accommodate three calcium ions (*10*, *13*), while the C2B domain binds two (*14*, *15*). However, the isolated C2 domains show no gross structural change when the Ca^{2+}-free and Ca^{2+}-bound states are compared (*16*); therefore, any structural change associated with full-length synaptotagmin function must rely on relative domain motions and not intradomain changes.

EXPERIMENTAL PROCEDURES

Protein Expression and Purification. Human synaptotagmin 1 C2A−C2B was obtained via PCR from a human hippocampal Quick-Clone cDNA library (Clontech). An 858-nucleotide fragment comprising Syt1 C2A−C2B residues 141−422 was directly cloned into PCR2.1 (Invitrogen), excised using *Bam*H1 and *Xho*1, and subsequently subcloned into pGEX4T-1 (GE-Healthcare). DNA sequence analysis confirmed insertion in the correct reading frame with respect to the GST fusion partner. The cytosolic fragment of human synaptotagmin 1, containing only the cytosolic C2A and C2B, was overexpressed in *Escherichia coli* as a GST fusion protein (*17*) and purified.

Diffraction Data Collection. Data were collected at the Stanford Synchrotron Radiation Laboratory (SSRL) on beamline 11-1 at a wavelength of 0.97 Å (Table 1). The data sets were collected at 100 K using an ADSC image plate detector. Data were integrated, reduced, and scaled using HKL2000 (*18*). The crystals were indexed in the orthorhombic space group $P2_12_12_1$; data statistics are summarized in Table 1.

Structure Determination and Refinement. Crystals were grown in the absence of Ca^{2+} as described elsewhere (*17*).

Table 1: Data Collection and Refinement Statistics for Syt1 C2AB

Data Collection	
space group	$P2_12_12_1$
cell dimensions	
a, *b*, *c* (Å)	82.3, 86.3, 147.2
α, *β*, *γ* (deg)	90, 90, 90
resolution (Å)	50−2.7 (2.85−2.7)[a]
R_{sym} or R_{merge} (%)	8.6 (44)[a]
$I/\sigma(I)$	13 (2.8)[a]
completeness (%)	99.5 (99.9)[a]
redundancy	4.0 (4.0)[a]
Refinement	
resolution (Å)	46−2.7
no. of reflns	29304
R_{work}/R_{free}	25.3/23.0
no. of atoms	
protein	4514
ligand/ion	8
water	43
B factors (Å^2)	chain A + chain B
protein	47
ligand/ion	40.5
water	33
rms dev	
bond lengths (Å)	0.007
bond angles (deg)	1.3
Ramachandran Map[b]	
most favored regions (%)	89.2
additional allowed regions (%)	10.8
generously allowed regions (%)	0
disallowed regions (%)	0

[a] All data were collected from a single frozen crystal. Values in parentheses are for the highest-resolution shell. [b] For chains (A + B) in the ASU.

The structure of synaptotagmin 1 C2A−C2B was solved via molecular replacement using Phaser (*19*) using diffraction data collected from one crystal to 2.7 Å (Table 1). Initial model coordinates were obtained using the C2A domain (PDB code 1BYN) and the C2B domain (PDB code 1TJX). Model building was done with Coot (*20*). Refinement of the model was carried out with CNS with a random subset of

all data set aside for calculation of R_{free} (10%). Manual adjustments to the models were carried out with Coot. After refinement of the protein was complete, solvent molecules were assessed followed by manual adjustments. Chloride ions were assigned on the basis of the chemical environment, the refined *B* factor vs that of the other water molecules, and the available coordination potential. The structure of C2A−C2B was verified by examining a simulated annealing omit map generated with CNS v1.2 (Figure S1 in the Supporting Information). There were no residues in disallowed regions of the Ramachandran map (Table 1). All figures were rendered with Pymol (*21*).

RESULTS AND DISCUSSION

To examine whether the C2 domains of Syt1 interact with each other prior to a Ca^{2+}-dependent switch, we solved the 2.7 Å crystal structure (Table 1) of the complete cytosolic portion of Syt1 C2AB (Figure 1A). The protein was purified in the presence of EDTA, and no additional sources of divalent cations were added at the crystallization stage. We show that the two C2 domains of Syt1 are capable of forming specific interdomain interactions between amino acids on the H-A helix of C2B and residues on loops 1−3 of C2A. These interactions distort loop 3 of C2A relative to the conformation of the same loop in the isolated C2A domain. The two Syt1 C2AB molecules in the asymmetric unit show the same interactions; further, there are no crystal contacts that would artificially distort loop 3 of C2A. Therefore, this orientation likely represents the interdomain interactions that are present in Syt1 prior to the Ca^{2+} flux.

Overall Structure of Syt1 C2A−C2B. As this is the first atomic structure of Syt1 C2A−C2B, we have defined the extent of the C2 domains, as well as the linker, on the basis of their structural contributions to the overall fold of the protein. The residue numbering used throughout will correspond to the well-described rat Syt1 protein sequence, unless otherwise noted. The human Syt1 primary sequence is essentially identical to the rat/mouse sequence with the exception of one additional amino acid at the extreme N-terminus. We define a residue as part of the C2 domain "motif" if it interacts with other amino acids in the fold either by contributing a hydrogen bond to peptide backbone residues or by packing next to other secondary structural elements within the C2 domain. By this definition, the C2A domain extends from residue Leu-142 to Gln-263. The nine-residue linker extends from Ser-264 to Lys-272. The C2B domain of Syt1 extends from Leu-273 to Lys-423. The two C2 domains of human Syt1 share ∼33% primary sequence identity; however, C2B possesses additional residues that correspond to two α-helices near its C-terminus (H-A and H-B) (*14*, *15*). Primary sequence alignment of all the known human isoforms of synaptotagmin show that while the H-A helix is a common feature of most C2B domains, the H-B helix is present in only a subset of the paralogues (Figure 4).

Variable Loop Conformations of Syt1 C2A−C2B. Syt1 crystallizes as a dimer in the asymmetric unit. While we do not ascribe physiological meaning to the dimer itself, it does allow us to compare the loop structures between the two molecules of the asymmetric unit and the isolated C2 domains, within the limits of our resolution range and refinement protocol. In this Syt1 C2A−C2B crystal structure, the tertiary folds of both C2B domains are similar. Further, the fold of the C2B domains in our crystal is similar to that of the isolated C2B domain (*14*, *15*). The rmsd between the isolated C2B structure and the C2B domain in the context of the tandem C2 domains is 0.58 Å over all Cα residues. We conclude that no part of C2B undergoes significant structural change in the context of C2A−C2B.

When the two C2A domains present in the crystallographic asymmetric unit are compared to the isolated Syt1 C2A domain, there are significant differences in loops 1 and 3 (Figure 2B). These differences are partly due to the hingelike behavior of the loops in the unliganded state of the C2A domains in this crystal. Because of this hinge motion, Asp-172, one of the Ca^{2+}-binding residues on loop 1, was traced near the surface of the domain in one molecule, while the other conformation was directed in toward the Ca^{2+}-binding pocket (Figure 2A). The flexible nature of this loop was not observed for C2B, as both loops 1 and 3 appear to be well ordered in this crystal form.

The structural variations observed in loop 3 of C2A are evident when C2A−C2B is compared to either the isolated Syt1 C2A crystal structure (with no Ca^{2+}) (*9*) or Syt1 C2A with saturating Ca^{2+} (*22*) (Figure 2A). Regardless of the Ca^{2+} occupancy of the isolated C2A domain, the absolute position of loop 3 resembles that of the C2B domains; consequently, the Ca^{2+}-associating residues are oriented to bind calcium ion. However, in the C2A−C2B domain structure, this loop is restrained in an alternate conformation that is not consistent with the typical Ca^{2+} coordination geometry previously observed in the C2A domain. Typical calcium ion coordination by proteins utilizes a pentagonal bipyramidal array with an average 2.4 Å separation to oxygen atoms (*23*). This type of coordination is not possible while loop 3 is restrained by C2B. Therefore, given this geometry, one would not expect C2A to bind Ca^{2+} in the presence of C2B while in the closed conformation.

Modulation of Loop 3 in C2A. The stabilization of loop 3 in this alternate position involves key residues in the "...SDPYVKV..." sequence in C2A. This motif is highly conserved across many C2 sequences, so the potential to modulate loop 3 may be a common feature of the C2 domain (Figure 4). The Ca^{2+}-binding conformation of loop 3 in the isolated C2A domain is stabilized by a hydrogen bond between His-237 (H-bond acceptor) and the central Tyr in the sequence motif listed above (Tyr-180, the H-bond donor) (Figure 5B). However, in the human Syt1 C2A−C2B structure, an alternate interaction of His-237 with Thr-406 in the C2B domain allows loop 3 in C2A to collapse (Figure 5A). The importance of this Tyr on β-sheet 3 at this special position is supported by genetic evidence.

In the *Drosophila* Syt1 C2B domain, the mutation of Tyr-364 to Asn (known as the AD3 mutation) abolishes Ca^{2+}-evoked neurotransmitter release (*24*, *25*). By raising extracellular Ca^{2+} from 400 μM to 6 mM, exocytosis in these mutants can be partially rescued (*26*). This implies that the divalent cation-binding machinery is still present in C2B, but the affinity for Ca^{2+} has been drastically altered. The marked phenotype of this mutation clearly illustrates that there is a direct link between Tyr-364 and Ca^{2+} affinity. To understand the relationship between our structure of human Syt1 C2AB and this mutation in *Drosophila*, we computed

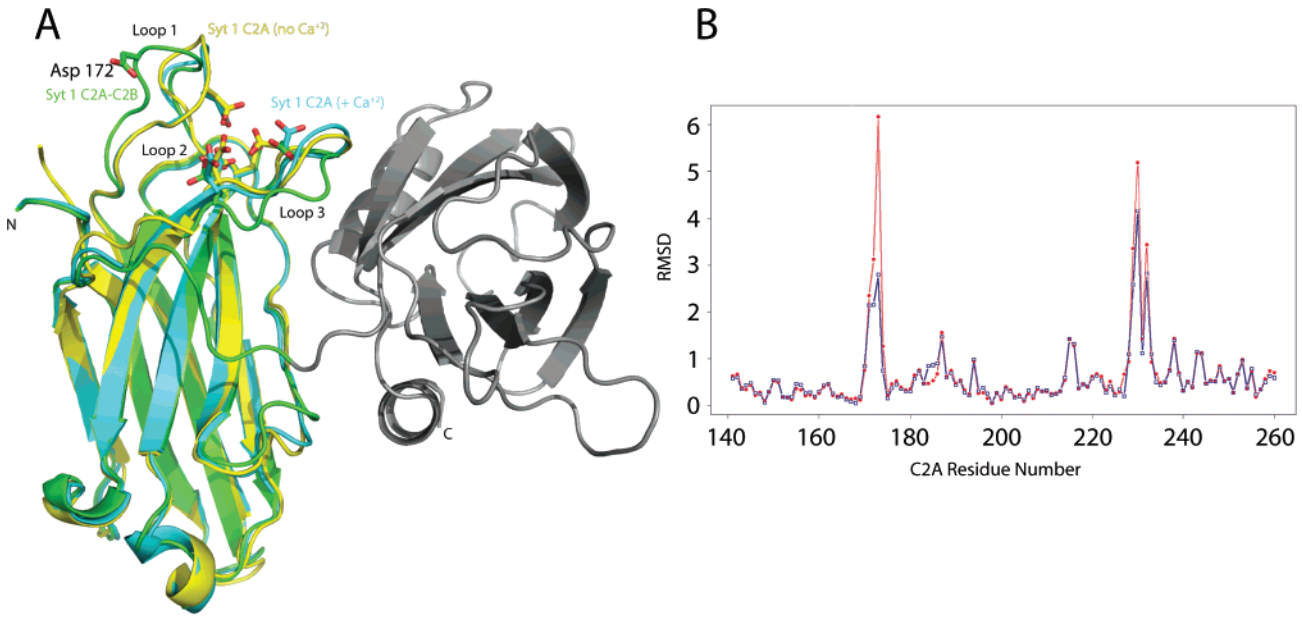

FIGURE 2: (A) Superposition of the isolated Syt1 C2A domain (PDB code 1RSY, yellow), the Ca^{2+}-saturated Syt1 C2A domain (PDB code 1BYN, cyan), and C2A (in this crystal structure, green). The C2B domain is shown in gray. The Ca^{2+}-binding residues for the C2A domain are shown as sticks. The more distal position of Asp-172 in the C2AB structure is highlighted. The N- and C-termini of the synaptotagmin C2A−C2B protein are labeled as N and C. (B) Rmsd plot over all Cα atoms between each of the C2A domains in the C2A−C2B crystal structure and the isolated C2A domain (1RSY). The red curve is the C2A domain of molecule A vs 1RSY, and the blue curve represents molecule B vs 1RSY. The residue ranges corresponding to loops 1 and 3 are shown by the bars above the major peaks. NCS restraints were used throughout the refinement with the exception of residues of loops 1 and 3 in C2A, where considerable differences in the path of the loops were observed.

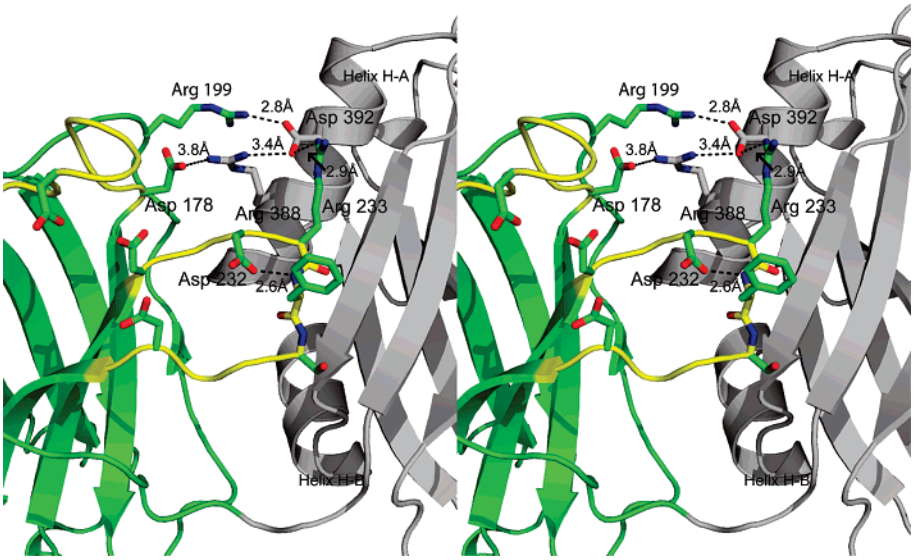

FIGURE 3: Stereoview of the C2A−C2B interdomain interactions. C2A is rendered in green ribbons, and C2B is rendered in gray on the right. Interacting residues are labeled according to the rat Syt1 numbering scheme. Also shown is the intradomain interaction between Asp-232 in C2A and the backbone amide of Phe-234.

a homology model of *Drosophila* Syt1 C2B based on the primary structure alignment of all available Syt1 orthologues and our X-ray structure of human Syt1 C2B (data not shown). In this model, Tyr-364 in *Drosophila* Syt1 C2B is homologous to the Tyr-180 position in the human Syt1 C2A domain. The model also predicts that Ser-423 (on loop 3) serves as the H-bond acceptor of Tyr-364 (β-sheet 3). We hypothesize that the phenotype of the AD3 mutation results from the removal of the hydrogen bond between Tyr-364 on β-sheet 3 and Ser-423 on loop 3 of *Drosophila* C2B, thus collapsing loop 3 of C2B. The collapse of loop 3 repositions the Ca^{2+}-binding residues, thereby increasing the amount of Ca^{2+} needed to rescue function. A homologous process may be occurring in human Syt1 C2A by the close proximity of C2B. Since C2B reorients His-237, the H-bonding acceptor to Tyr-180, the same loss of Ca^{2+} affinity could be occurring in C2A (Figure 5B). Therefore, the AD3 mutation may mimic the behavior of the wild-type C2A domain under the influence of C2B.

Interdomain Interactions. The conformation of loop 3 in C2A is restrained exclusively by the interdomain interactions described below. As there are no significant contacts made by crystallographically related molecules, we conclude that the interactions we observe are possible in the native protein.

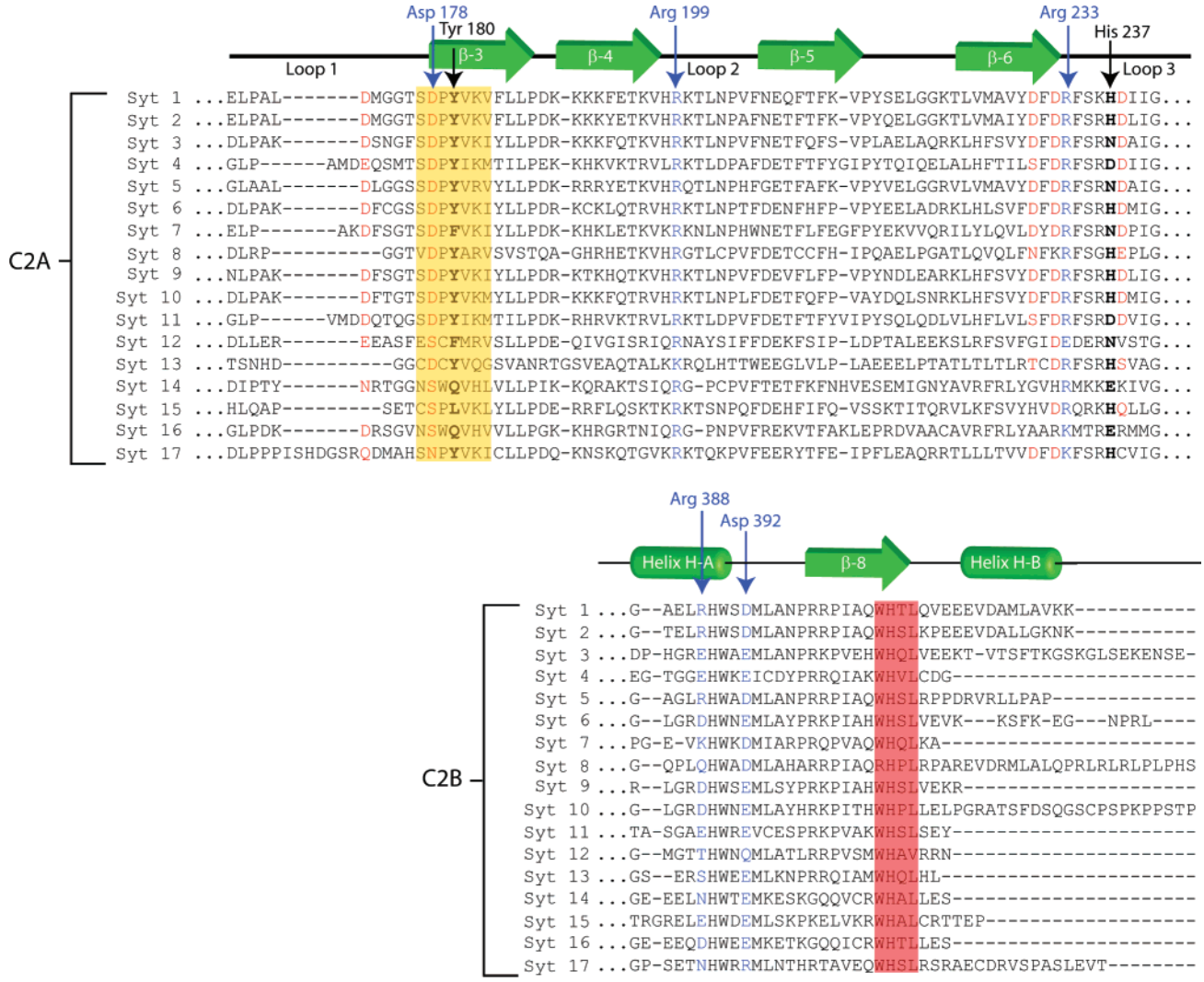

FIGURE 4: ClustalW alignment of the reported human synaptotagmin paralogues. The green arrows correspond to β-sheet structures in the C2 domains. The green tubes represent α-helical regions in the C2B domain. The top half of the alignment shows residues Glu-169 to Gly-242 in human Syt1 C2A; the bottom half only shows residues Gly-385 to Lys-422 in C2B. Residues highlighted in red correspond to acidic residues in Syt1 C2A known to coordinate Ca^{2+}. Red residues in Syt2-17 share homologous positions and, in most cases, contribute to Ca^{2+} binding in those isoforms. The residues highlighted in the yellow box are those in β-strand 3 implicated in the modulated loop 3 structure of Syt1. The other residues homologous to the "SDPYVKV" motif within the yellow box may play similar roles in other paralogues. Residues in blue were observed forming salt bridges between C2A and C2B in Syt1. Residues boxed in red comprise the conserved "WHxL" motif.

Almost all of the amino acid interactions that link C2A with C2B are located on the H-A α-helix of C2B and loops 1−3 of the divalent cation-binding pocket of C2A (Figure 3). Arg-388 on the H-A helix of C2B forms a salt-bridge interaction with Asp-178 located on loop 1 of C2A. In previous structural analysis, Asp-178 contributes a single carbonyl oxygen to the highest affinity Ca^{2+}-binding site (*9*). When Asp-178 is mutated to Asn in the isolated C2A domain, Ca^{2+} binding is disrupted (*27*, *28*). Since the observed interaction between Asp-178 and Arg-388 directly links C2B to calcium ion-binding residues in C2A, it is tempting to conclude that this interaction may represent a switch or trigger to link Ca^{2+} occupancy to Syt1 function. However, when this mutation was introduced into *Drosophila*, no significant phenotype was observed (*29*). While Asp-178 is certainly important to the overall function of Syt1, it is clear that this residue is not solely responsible for the interactions with C2B. A second interdomain interaction observed between C2A and C2B is contributed by Asp-392 of C2B. This residue forms a bifurcated salt bridge between Asp-392 and Arg-199 on loop 2 in C2A and between Asp-392 and Arg-233 on loop 3. Arg-199 is also a notable residue as it participates in several activities of C2A (interactions with phospholipid (*12*) and SNARE components) and is a contributor to the electrostatic switch of C2A (*30*).

Consequences of the Tandem Arrangement. Most C2 domains share two common functions: The first is as an adapter module that links a client protein or a neighboring motif to a phospholipid bilayer through the hydrophobic residues at the tips of the C2 domain (*31*), and the second function is mediated through the effector-binding polybasic regions (*32*, *33*). In the closed conformation, the association with C2B affects residues that mediate both of these activities. The polybasic region of C2A is composed of four contiguous Lys residues at the amino terminus of the β-strand and three basic amino acids at the carboxy terminus of β-strand 4. While the biological function of the polybasic domain of C2A in Syt1 function is not as clear as that of C2B, this region of C2A is almost completely occluded by its interaction with C2B. Upon forming the closed conforma-

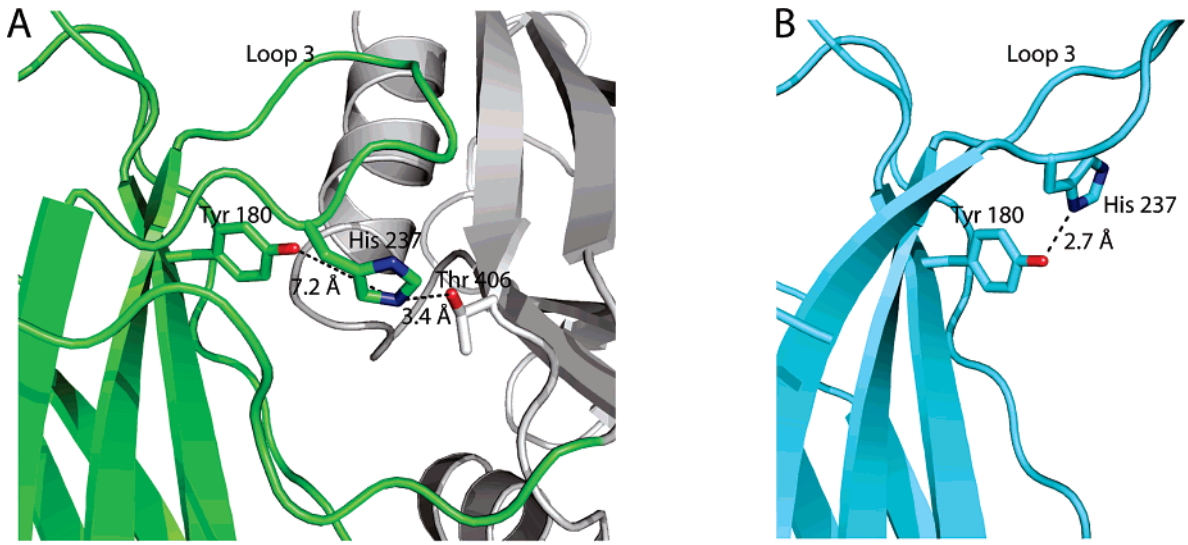

FIGURE 5: The rotameric position of His-237 depends on whether C2A is coupled to C2B. (A) The His-237 residue can pair with Thr-406 in C2B. C2B is rendered as gray helices and ribbons. (B) Hydrogen-bonding partner of His-237 in the isolated C2A domain of rat synaptotagmin 1 (1RSY).

tion, ~890 Å^2 of solvent-accessible surface area is buried per C2 domain. This degree of domain contact is comparable to that of other observed protein dimer interfaces and is indicative of associations that require weaker interactions (*34*). Thus, the closed conformation of Syt1 may obstruct premature interactions with effectors such as phospholipids, syntaxin, or the voltage-gated Ca^{2+} channel (*30*, *35*, *36*). Another notable feature of C2B is the highly conserved "WH*x*L" sequence in C2B. This motif has been implicated in docking events and neurexin binding of Syt1 in the synapse (*37*). In the closed conformation of Syt1 C2A−C2B, ~40% of the solvent-exposed surface area of the "...WHTL..." motif is occluded by the C2A−C2B interface. Most of this surface area is lost by burying Trp-405 within the interface. If this sequence does mediate the docking of synaptotagmin to the plasma membrane through a specific receptor, then it would be unable to do so while in this closed conformation.

Implications for Other Synaptotagmin Orthologues. The human genome possesses genes for at least 17 distinct synaptotagmin proteins (Figure 4). The excessive redundancy of the Syt orthologues is either due to the critical nature of Syt in regulated exocytosis (*38*) or as part of an intricate addressing system that allows for the temporal and spatial fine-tuning of fusion between specific vesicles and specific membrane targets in various cell types (*39*). The residues that we observe at the interface between C2A and C2B are present in many of the other isoforms, but not all. Therefore, it is conceivable that this C2A−C2B domain orientation is unique to Syt1. The position of C2A relative to C2B may vary by homologue depending on the particular biological requirements of the cell.

CONCLUSION

The C2A and C2B domains of Syt1 are related by a ~108° rotation about the linker axis. This is in contrast to the more "open" conformation of Mg^{2+}-bound Syt3 C2A−C2B where there are no interdomain interactions between domains and the phospholipid-binding loops directly face one another (Figure 1B) (*6*). NMR analysis of Syt1 C2A−C2B concluded that, like Syt3, the domains of Syt1 can be separate and noninteracting (*5*). However, we clearly observe extensive interactions between domains. To rationalize these seemingly disparate results, we hypothesize that Syt1 possesses an open conformation and a closed conformation that are critical to its function. The closed form may be required for regulating the activity of Syt1 prior to fulfilling its role in exocytosis, while the open form may be required for effector interaction during the final stages of exocytosis.

We propose that, while still in this closed conformation, C2B·Ca^{2+} initially localizes to the membrane surface and may begin to associate with phospholipid membranes and other factors required for exocytosis (*40*). As the Ca^{2+}/phospholipid-binding loops of C2B are already in a conformation amenable to phospholipid interaction, it is reasonable to assume that C2B will behave as a phospholipid-binding module to initially localize the Ca^{2+} sensor to the target membrane. This may explain why C2B appears more essential to the Syt1 protein, as it could be the first domain capable of responding to cytosolic Ca^{2+} gradients (*41*). At some point, the C2A domain must detach from C2B under the influence of a trigger. We predict that the trigger will be a threshold Ca^{2+} concentration, but phospholipid interaction, effector protein binding, or some combination of the three may initiate the transformation of the Syt1 molecule to an open conformation. Next, the divalent cation-binding loops 1 and 3 of C2A will attain their final conformation as calcium ions occupy binding sites (*40*). The final phase of synaptotagmin action is presently unclear, as it may involve a direct mechanism of phospholipid demixing that leads to fusion, or the protein will set the stage for another component to facilitate the final step. This model of Syt1 C2AB also suggests a mechanism whereby the two C2 domains of synaptotagmin may act on the target membrane in series rather than in parallel, thereby providing a true structural trigger. Consequently, C2A may only attain its final Ca^{2+}-occupied, membrane-binding competent structure during the final few microseconds prior to exocytosis. Defining the structural basis for the interactions of synaptotagmin 1, as well as other isoforms, with SNARE components and phospholipid bilayers will be the focus of future studies.

ACKNOWLEDGMENT

We thank Drs. Betsy Goldsmith and Andres Oberhauser for help with the manuscript. We also acknowledge Jason Vertrees for help with the statistical plotting software "R".

SUPPORTING INFORMATION AVAILABLE

Representative electron density, http://xray.utmb.edu/~sutton/biochemistry_el_density_map.pdf, $2mF_o - DF_c$ simulated annealing (SA) composite omit map (at the 1.0σ contour level) of the interfacial residues between Syt1 C2A and C2B (residues in green localize to the C2A domain, whereas the gray residues localize to the C2B domain). This material is available free of charge via the Internet at http://pubs.acs.org.

REFERENCES

1. Dennison, S. M., Bowen, M. E., Brunger, A. T., and Lentz, B. R. (2006) Neuronal SNAREs do not trigger fusion between synthetic membranes but do promote PEG-mediated membrane fusion, *Biophys. J. 90*, 1661−1675.
2. Weber, T., Zemelman, B. V., McNew, J. A., Westermann, B., Gmachl, M., Parlati, F., Sollner, T. H., and Rothman, J. E. (1998) SNAREpins: minimal machinery for membrane fusion, *Cell 92*, 759−772.
3. Chapman, E. R. (2002) Synaptotagmin: a Ca^{2+} sensor that triggers exocytosis?, *Nat. Rev. Mol. Cell Biol. 3*, 498−508.
4. Rickman, C., Archer, D. A., Meunier, F. A., Craxton, M., Fukuda, M., Burgoyne, R. D., and Davletov, B. (2004) Synaptotagmin interaction with the syntaxin/SNAP-25 dimer is mediated by an evolutionarily conserved motif and is sensitive to inositol hexakisphosphate, *J. Biol. Chem. 279*, 12574−12579.
5. Arac, D., Chen, X., Khant, H. A., Ubach, J., Ludtke, S. J., Kikkawa, M., Johnson, A. E., Chiu, W., Sudhof, T. C., and Rizo, J. (2006) Close membrane-membrane proximity induced by Ca^{2+}-dependent multivalent binding of synaptotagmin-1 to phospholipids, *Nat. Struct. Mol. Biol. 13*, 209−217.
6. Sutton, R. B., Ernst, J. A., and Brunger, A. T. (1999) Crystal structure of the cytosolic C2A-C2B domains of synaptotagmin III. Implications for Ca^{+2}-independent snare complex interaction, *J. Cell Biol. 147*, 589−598.
7. Damer, C. K., and Creutz, C. E. (1994) Synergistic membrane interactions of the two C2 domains of synaptotagmin, *J. Biol. Chem. 269*, 31115−31123.
8. Hui, E., Bai, J., and Chapman, E. R. (2006) Ca^{2+}-triggered simultaneous membrane penetration of the tandem C2-domains of synaptotagmin I, *Biophys. J. 91*, 1767−1777.
9. Sutton, R. B., Davletov, B. A., Berghuis, A. M., Sudhof, T. C., and Sprang, S. R. (1995) Structure of the first C2 domain of synaptotagmin I: a novel Ca^{2+}/phospholipid-binding fold, *Cell 80*, 929−938.
10. Shao, X., Davletov, B. A., Sutton, R. B., Sudhof, T. C., and Rizo, J. (1996) Bipartite Ca^{2+}-binding motif in C2 domains of synaptotagmin and protein kinase C, *Science 273*, 248−251.
11. Chae, Y. K., Abildgaard, F., Chapman, E. R., and Markley, J. L. (1998) Lipid binding ridge on loops 2 and 3 of the C2A domain of synaptotagmin I as revealed by NMR spectroscopy, *J. Biol. Chem. 273*, 25659−25663.
12. Chapman, E. R., and Davis, A. F. (1998) Direct interaction of a Ca^{2+}-binding loop of synaptotagmin with lipid bilayers, *J. Biol. Chem. 273*, 13995−14001.
13. Sutton, R. B., and Sprang, S. R. (1998) Structure of the protein kinase C-β phospholipid-binding C2 domain complexed with Ca^{2+}, *Structure 6*, 1395−1405.
14. Cheng, Y., Sequeira, S. M., Malinina, L., Tereshko, V., Sollner, T. H., and Patel, D. J. (2004) Crystallographic identification of Ca^{2+} and Sr^{2+} coordination sites in synaptotagmin I C2B domain, *Protein Sci. 13*, 2665−2672.
15. Fernandez, I., Arac, D., Ubach, J., Gerber, S. H., Shin, O., Gao, Y., Anderson, R. G., Sudhof, T. C., and Rizo, J. (2001) Three-dimensional structure of the synaptotagmin 1 C2B-domain: synaptotagmin 1 as a phospholipid binding machine, *Neuron 32*, 1057−1069.
16. Rizo, J., and Sudhof, T. C. (1998) C2-domains, structure and function of a universal Ca^{2+}-binding domain, *J. Biol. Chem. 273*, 15879−15882.
17. Montes, M., Fuson, K. L., Sutton, R. B., and Robert, J. J. (2006) Purification, crystallization and X-ray diffraction analysis of human synaptotagmin 1 C2A-C2B, *Acta Crystallogr. F*.
18. Otwinowski, Z., and Minor, W. (1997) Processing of X-ray Diffraction Data Collected in Oscillation Mode, in *Methods in Enzymology, Macromolecular Crystallography, part A* (Carter, C., and Sweet, R., Eds.) pp 307−326, Academic Press, New York.
19. McCoy, A. J., Grosse-Kunstleve, R. W., Storoni, L. C., and Read, R. J. (2005) Likelihood-enhanced fast translation functions, *Acta Crystallogr. D61*, 458−464.
20. Emsley, P., and Cowtan, K. (2004) Coot: model-building tools for molecular graphics, *Acta Crystallogr. D60*, 2126−2132.
21. DeLano, W. L. (2002) *The PyMOL Molecular Graphics System*, DeLano Scientific, Palo Alto, CA.
22. Shao, X., Fernandez, I., Sudhof, T. C., and Rizo, J. (1998) Solution structures of the Ca^{2+}-free and Ca^{2+}-bound C2A domain of synaptotagmin I: does Ca^{2+} induce a conformational change?, *Biochemistry 37*, 16106−16115.
23. Strynadka, N. C., and James, M. N. (1989) Crystal structures of the helix-loop-helix calcium-binding proteins, *Annu. Rev. Biochem. 58*, 951−998.
24. Okamoto, T., Tamura, T., Suzuki, K., and Kidokoro, Y. (2005) External Ca^{2+} dependency of synaptic transmission in *Drosophila* synaptotagmin I mutants, *J. Neurophysiol. 94*, 1574−1586.
25. DiAntonio, A., Parfitt, K. D., and Schwarz, T. L. (1993) Synaptic transmission persists in synaptotagmin mutants of *Drosophila*, *Cell 73*, 1281−1290.
26. Littleton, J. T., Bai, J., Vyas, B., Desai, R., Baltus, A. E., Garment, M. B., Carlson, S. D., Ganetzky, B., and Chapman, E. R. (2001) Synaptotagmin mutants reveal essential functions for the C2B domain in Ca^{2+}-triggered fusion and recycling of synaptic vesicles in vivo, *J. Neurosci. 21*, 1421−1433.
27. Fernandez-Chacon, R., Konigstorfer, A., Gerber, S. H., Garcia, J., Matos, M. F., Stevens, C. F., Brose, N., Rizo, J., Rosenmund, C., and Sudhof, T. C. (2001) Synaptotagmin I functions as a calcium regulator of release probability, *Nature 410*, 41−49.
28. Ubach, J., Zhang, X., Shao, X., Sudhof, T. C., and Rizo, J. (1998) Ca^{2+} binding to synaptotagmin: how many Ca^{2+} ions bind to the tip of a C2-domain? *EMBO J. 17*, 3921−3930.
29. Robinson, I. M., Ranjan, R., and Schwarz, T. L. (2002) Synaptotagmins I and IV promote transmitter release independently of Ca^{2+} binding in the C(2)A domain, *Nature 418*, 336−340.
30. Shao, X., Li, C., Fernandez, I., Zhang, X., Sudhof, T. C., and Rizo, J. (1997) Synaptotagmin-syntaxin interaction: the C2 domain as a Ca^{2+}-dependent electrostatic switch, *Neuron 18*, 133−142.
31. Edwards, A. S., and Newton, A. C. (1997) Regulation of protein kinase C βII by its C2 domain, *Biochemistry 36*, 15615−15623.
32. Grass, I., Thiel, S., Honing, S., and Haucke, V. (2004) Recognition of a basic AP-2 binding motif within the C2B domain of synaptotagmin is dependent on multimerization, *J. Biol. Chem. 279*, 54872−54880.
33. Chapman, E. R., Desai, R. C., Davis, A. F., and Tornehl, C. K. (1998) Delineation of the oligomerization, AP-2 binding, and synprint binding region of the C2B domain of synaptotagmin, *J. Biol. Chem. 273*, 32966−32972.
34. Jones, S., and Thornton, J. M. (1996) Principles of protein-protein interactions, *Proc. Natl. Acad. Sci. U.S.A. 93*, 13−20.
35. Charvin, N., L'Eveque, C., Walker, D., Berton, F., Raymond, C., Kataoka, M., Shoji-Kasai, Y., Takahashi, M., De Waard, M., and Seagar, M. J. (1997) Direct interaction of the calcium sensor protein synaptotagmin I with a cytoplasmic domain of the alpha1A subunit of the P/Q-type calcium channel, *EMBO J. 16*, 4591−4596.
36. Cohen, R., Schmitt, B. M., and Atlas, D. (2005) Molecular identification and reconstitution of depolarization-induced exocytosis monitored by membrane capacitance, *Biophys. J. 89*, 4364−4373.
37. Fukuda, M., Moreira, J. E., Liu, V., Sugimori, M., Mikoshiba, K., and Llinas, R. R. (2000) Role of the conserved WHXL motif in the C terminus of synaptotagmin in synaptic vesicle docking, *Proc. Natl. Acad. Sci. U.S.A. 97*, 14715−14719.
38. Pang, Z. P., Shin, O. H., Meyer, A. C., Rosenmund, C., and Sudhof, T. C. (2006) A gain-of-function mutation in synaptotag-

min-1 reveals a critical role of Ca^{2+}-dependent soluble N-ethylmaleimide-sensitive factor attachment protein receptor complex binding in synaptic exocytosis, *J. Neurosci. 26*, 12556−12565.

39. McNew, J. A., Parlati, F., Fukuda, R., Johnston, R. J., Paz, K., Paumet, F., Sollner, T. H., and Rothman, J. E. (2000) Compartmental specificity of cellular membrane fusion encoded in SNARE proteins, *Nature 407*, 153−159.
40. Kertz, J. A., Almeida, P. F., Frazier, A. A., Berg, A. K., and Hinderliter, A. (2007) The cooperative response of synaptotagmin I C2A. A hypothesis for a Ca^{2+}-driven molecular hammer, *Biophys. J. 92*, 1409−1418.
41. Nishiki, T., and Augustine, G. J. (2004) Dual roles of the C2B domain of synaptotagmin I in synchronizing Ca^{2+}-dependent neurotransmitter release, *J. Neurosci. 24*, 8542−8550.

BI701651K